

# Strong Evidence of Normal Heat Conduction in a one-Dimensional Quantum System

KEIJI SAITO

*Department of Applied Physics, School of Engineering  
University of Tokyo, Bunkyo-ku, Tokyo 113-8656, Japan*

PACS. 05.60.Gg – Quantum transport.  
PACS. 05.30.-d – Quantum statistical mechanics.  
PACS. 05.70.Ln – Nonequilibrium and irreversible thermodynamics.

**Abstract.** – We investigate how the normal energy transport is realized in one-dimensional quantum systems using a quantum spin system. The direct investigation of local energy distribution under thermal gradient is made using the quantum master equation, and the mixing properties and the convergence of the Green-Kubo formula are investigated when the number of spin increases. We find that the autocorrelation function in the Green-Kubo formula decays as  $\sim t^{-1.5}$  to a finite value which vanishes rapidly with the increase of the system size. As a result, the Green-Kubo formula converges to a finite value in the thermodynamic limit. These facts strongly support the realization of Fourier heat law in a quantum system.

The Fourier heat law is one of the most important properties in the nonequilibrium thermodynamics. It states that the heat current per volume is proportional to the thermal gradient. Microscopic dynamical origin for the realization of Fourier heat law has been actively studied using many Hamiltonian systems [1, 2, 3]. In the complete harmonic chain, no global thermal gradient appears, and local equilibrium is not realized, which are attributed to the lack of scattering between modes [1, 4]. In an isotropic  $d$ -dimensional classical Fermi-Pasta-Ulam (FPU) system which has the nonlinear potential term, the mixing property satisfies because the auto-correlation function of the energy current roughly decays as  $t^{-d/2}$ . However due to its slow relaxation of the current fluctuation, the Green-Kubo formula diverges in the one- and two-dimensional systems which causes an anomalous energy transport [2, 5].

In low dimensional systems, most of the problems preventing a normal thermal conduction arises from a slow fluctuation of energy current, including the failure of mixing property. This situation is also the case in the quantum systems. Many integrable one-dimensional systems show the failure of mixing property. In the isotropic Heisenberg chain, the energy current operator commutes with the Hamiltonian, which trivially causes the failure of mixing property and the abnormal energy transport [6]. The recent experiments confirmed a such ballistic heat transport in  $\text{Sr}_2\text{CuO}_3$  [7] and  $\text{CuGeO}_3$  [8] which are described by the isotropic Heisenberg chain.

In this paper, we study how the normal thermal conduction in a one-dimensional quantum system is realized in microscopic point of view. In quantum systems, the dynamical origins of

normal thermal conduction and the related quantum effects are not enough understood [3,9]. In classical systems, *chaos* characterized by the sensitivity to the initial state can be induced by nonlinearities and can play a crucial role for the mixing property. However such *chaos* cannot be induced by a linear Schrödinger equation in quantum systems [10]. In spite of such discrepancies in dynamics, the Fourier heat law can be realized in quantum systems. We show the strong evidence of the normal thermal conduction in a one-dimensional quantum spin system by direct investigation of properties under thermal gradient and the Green-Kubo formula. We find that the autocorrelation function in the Green-Kubo formula approximately decays as  $t^{-1.5}$ . Thus the mixing property is satisfied and the formula converges.

We consider the tractable simple quantum system whose Hamiltonian is described as,

$$\mathcal{H} = \sum_{\ell=1}^{N_1} J \sigma_{\ell}^z \sigma_{\ell+1}^z + D (\sigma_{\ell}^z \sigma_{\ell+1}^x - \sigma_{\ell}^x \sigma_{\ell+1}^z) + \Gamma \sum_{\ell=1}^N \sigma_{\ell}^x + H \sum_{\ell=1}^N \sigma_{\ell}^z, \quad (1)$$

where  $\sigma_{\ell}^{\alpha}$  ( $\alpha = x, y, z$ ) is the  $\alpha$  component of the Pauli matrix at the  $\ell$ th site.  $N$  is the number of spin, and  $N_1$  is taken as  $N - 1$  for the open boundary condition and  $N$  for the periodic boundary condition, respectively. The first term is the nearest neighbor Ising interaction, and the second term is the Dzyaloshinsky-Moriya (DM) interaction, where the anisotropic vector is taken as  $\mathbf{D} = (0, D, 0)$  for the general form  $\mathbf{D} \cdot (\sigma_{\ell} \times \sigma_{\ell+1})$ . The third and fourth term are the Zeeman term of  $x$  and  $z$  direction, respectively.

This Hamiltonian shows the variety of symmetries by controlling parameters ( $J, D, \Gamma, H$ ). In the case of periodic boundary condition, there exists the translational symmetry  $\sigma_n \leftrightarrow \sigma_{n+\ell}$  ( $\ell = 1, \dots, N$ ). In the absence of the DM interaction, i.e,  $D = 0$ , the system has the reflection symmetry,  $\sigma_n \leftrightarrow \sigma_{N-n}$ . In the case of  $D = 0$  and  $H = 0$ , the system Hamiltonian is diagonalized by using free fermions through the Jordan-Wigner transformation [11]. When  $\Gamma = 0$  and  $H = 0$ , the system has the time reversal symmetry which yields the Kramers degeneracies. In many systems with symmetries, conserved quantities prevent a normal heat transport, so that the Green-Kubo formula diverges [6, 12].

As well known, level spectrum shows the universal statistics according to the nonintegrability of system [13]. We investigate the cumulative spacing distribution  $I(S)$  defined by  $I(S) = \int_0^S du P(u)$  for the energy spacing distribution  $P(u)$ . We show the distributions in Fig.1 for  $(J, D, \Gamma, H) = (0.2, 0.2, 0.2, -0.2)$  and  $(0.2, 0, 0.2, 0)$  with the open boundary condition  $N_1 = N - 1$ . The former system has no trivial symmetries, while the latter can be mapped into free-fermion. Points are numerical data by diagonalizing the Hamiltonian (1), and the lines are theoretical predictions, i.e., the Poisson distribution  $I(S) = 1 - \exp(-S)$  for integrable systems, and the Wigner distribution  $I(S) = 1 - \exp(-\pi S^2/4)$  for nonintegrable systems, respectively. The figure for the parameters  $(0.2, 0.2, 0.2, -0.2)$  shows the agreement between the numerical data and the Wigner surmise. For small spacing  $S \ll 1$ ,  $I(S)$  behaves as  $I(S) \propto S^{1.92 \pm 0.02}$ , which is very close to the Wigner distribution  $I(S) \propto S^2$ . This universal feature of spectrum indicates a complex dynamics of this system. Thus throughout this paper, we take the parameters as  $J = D = \Gamma = -H = 0.2$  [14].

In order to investigate properties of the energy transport under thermal gradient, the reservoirs of different temperatures are directly connected with the system at the both ends. Here we adopt the phonon reservoir with the Ohmic spectral density for which the master equation of the system is written as (see e.g., [4] and references therein);

$$\frac{\partial \rho(t)}{\partial t} = -i [\mathcal{H}, \rho(t)] - \lambda (\mathcal{L}_L \rho(t) + \mathcal{L}_R \rho(t)), \quad (2)$$

where the first term in the right-hand side corresponds to the pure quantum dynamics of the

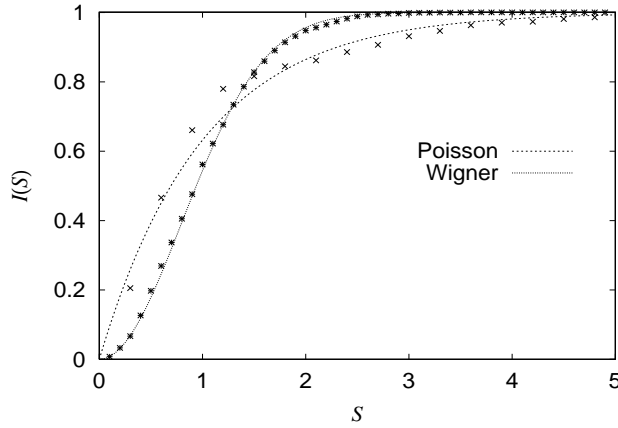


Fig. 1 – Cumulative level spacing distribution for  $N = 12$  with the open boundary condition. The asterisk and cross are for the cases of  $(J, D, \Gamma, H) = (0.2, 0.2, 0.2, -0.2)$  and  $(0.2, 0, 0.2, 0)$ , respectively. For small  $S$  in the former case,  $I(S)$  is approximately fitted by  $I(S) \propto S^{1.92 \pm 0.02}$ .

system, and  $\mathcal{L}_L$  and  $\mathcal{L}_R$  express the dissipative effects of the inverse temperature  $\beta_L$  at the left reservoir and  $\beta_R$  at the right reservoir, respectively. The parameter  $\lambda$  is the coupling strength. The dissipative term  $\mathcal{L}_\alpha$  ( $\alpha = L, R$ ) is given by  $\mathcal{L}_\alpha \rho(t) = \left( [X_\alpha, R_\alpha \rho(t)] + [X_\alpha, R_\alpha \rho(t)]^\dagger \right)$ , where  $X_L$  and  $X_R$  are the system's operators directly attached to the left and right reservoir, respectively. Here we take  $X_L = \sigma_1^z$  and  $X_R = \sigma_N^z$ . The operator  $R_\alpha$  is given by  $\langle k | R_\alpha | m \rangle = (E_k - E_m)(e^{\beta_\alpha(E_k - E_m)} - 1)^{-1} \langle k | X_\alpha | m \rangle$  in the representation diagonalizing the Hamiltonian (1) as  $\mathcal{H}|k\rangle = E_k|k\rangle$  and  $\mathcal{H}|m\rangle = E_m|m\rangle$ .

We first consider the energy profile defining the  $\ell$ th local Hamiltonian  $\mathcal{H}_\ell$ ;

$$\mathcal{H}_\ell = J\sigma_\ell^z \sigma_{\ell+1}^z + D(\sigma_\ell^z \sigma_{\ell+1}^x - \sigma_\ell^x \sigma_{\ell+1}^z) + \sum_{k=\ell}^{\ell+1} (\Gamma \sigma_k^x + H \sigma_k^z). \quad (3)$$

We numerically integrate the equation (2) and obtain the stationary density matrix  $\rho_{\text{st}}$  when the initial density matrix is taken as the canonical distribution of temperature  $1/\beta_R$ . The simulation was carried out by the fourth order Runge-Kutta method with the time step 0.01 for the parameters  $\beta_L = 0.5$ ,  $\beta_R = 0.2$ , and  $\lambda = 0.01$ . In Fig. 2, we show the energy profiles at the stationary state  $\text{Tr}(\rho_{\text{st}} \mathcal{H}_\ell)$  for  $N = 7, 8, 9$ , and 10. The two large circles are equilibrium energy values of inverse temperatures  $\beta_L$  and  $\beta_R$ , respectively.  $N = 10$  was the largest number within the present computational ability. The figure shows the profiles with a finite gradient which is the *sufficient condition* for the Fourier heat law, although we cannot enumerate the energy profile and energy current in the thermodynamic limit. The local energies at the both edges are different from the expectation values of the temperatures of reservoirs. This is attributed to the small coupling strength  $\lambda (= 0.01)$ . Actually we confirmed that for larger  $\lambda$  ( $\ll J, D$ ), the energy profile smoothly changes and these differences become smaller. We found the qualitatively same finite energy gradient in the case of smaller temperature difference  $\beta_L = 0.3$  and  $\beta_R = 0.2$ .

We next study the local energy distribution at the stationary state focusing on whether the local equilibrium is realized or not for the system of  $N = 10$ . The local equilibrium can

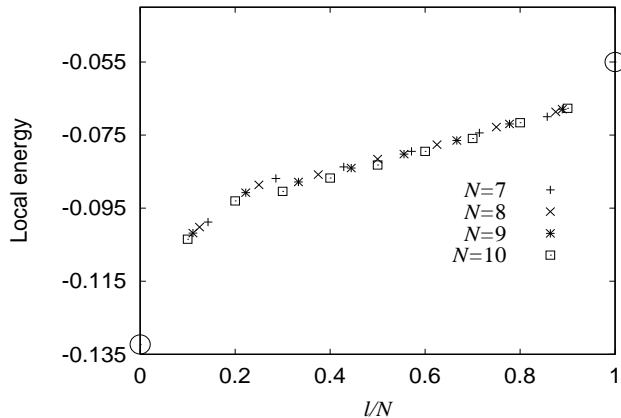


Fig. 2 – The energy profile at the stationary state for from  $N = 7$  to  $N = 10$ . The abscissa is the scaled spin number,  $l/N, l = 1, \dots, N - 1$ .

be realized even in finite size systems [15, 16]. We study the energy distribution of subsystems composed of two spins and four spins. We consider four local subsystems with two spins, i.e., the subsystems described by the local Hamiltonians,  $\mathcal{H}_2, \mathcal{H}_4, \mathcal{H}_6$ , and  $\mathcal{H}_8$ , and two local subsystems with four spins, i.e., the subsystems described by  $(\mathcal{H}_2 + \mathcal{H}_3)$  and  $(\mathcal{H}_6 + \mathcal{H}_7)$ . Temperatures at boundaries are set as  $(\beta_L, \beta_R) = (0.5, 0.2)$  for the former case and  $(\beta_L, \beta_R) = (0.3, 0.2)$  for the latter case. The  $l$ th local energy distribution  $P_\ell(\varepsilon_i)$  is calculated using the  $l$ th local reduced density matrix  $\rho_\ell$  as,

$$P_\ell(\varepsilon_i) = \langle i_\ell | \rho_\ell | i_\ell \rangle, \quad (4)$$

where  $|i_\ell\rangle$  is the  $i$ th eigenstate of the  $l$ th local subsystem Hamiltonian. The numbers of eigenstates are 4 and 16 for the cases of  $(\beta_L, \beta_R) = (0.5, 0.2)$  and  $(\beta_L, \beta_R) = (0.3, 0.2)$ , respectively. The  $l$ th local density matrix  $\rho_\ell$  is obtained by taking the trace for stationary density matrix  $\rho_{st}$  in the Hilbert space exclusive of spins which belong to the  $l$ th subsystem. In Fig.3, the energy distributions  $P_\ell(\varepsilon_i)$  are shown on the semi-log scale. The points linked by one line are the distribution at one local subsystem. With the increase of the subsystem number  $l$ , the gradient of the line becomes smaller. The distributions approximately take the exponential form. Thus this monotonic  $l$  dependence of gradient of energy distribution indicates that this system can be the *candidate* which satisfies the local equilibrium. We must note that the Ising and DM interaction between nearest neighbor local subsystems and the existence of finite energy flow can cause deviations of  $P_\ell(\varepsilon_i)$  from the exponential form.

Generally even if the energy profile is well scaled and the local equilibrium is realized, thermal conductivity can diverge in the thermodynamic limit due to the slow relaxation of energy currents mentioned in the introduction [16]. We now investigate whether this type of divergence occurs or not in the present system. The Green-Kubo formula is derived on the basis of the local equilibrium state. Since the present system is the candidate which satisfies the local equilibrium, we expect that the Green-Kubo formula quantitatively describes the thermal conductivity  $\kappa(\beta)$  in the thermodynamic limit. The Green-Kubo formula reads as,

$$\kappa(\beta) = \frac{\beta^2}{2N} \int_0^\infty du \langle \{ \hat{J}, \hat{J}(u) \} \rangle, \quad (5)$$

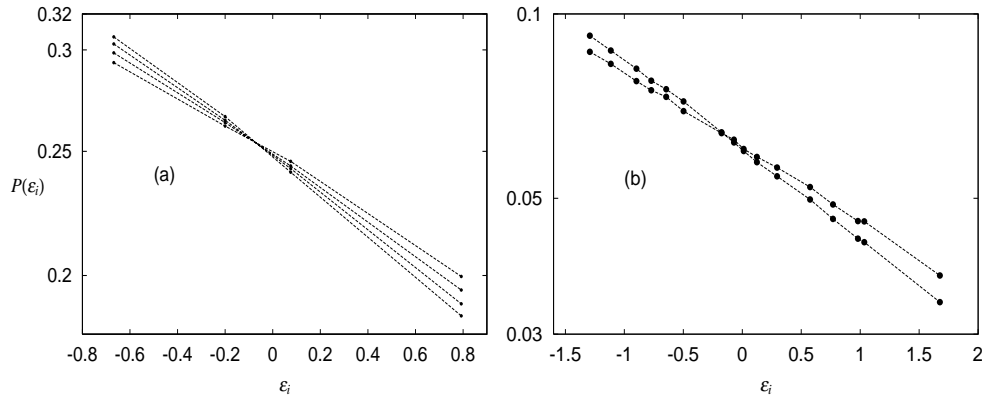


Fig. 3 – Local energy distribution for size  $N = 10$ . (a) Four local subsystems composed of two spins for  $(\beta_L, \beta_R) = (0.5, 0.2)$ . (b) Two local subsystems composed of four spins for  $(\beta_L, \beta_R) = (0.3, 0.2)$ .

where  $\{.,.\}$  means the anti-commutation relation, and  $\langle \dots \rangle$  is the equilibrium average at the inverse temperature  $\beta$ . The operator  $\hat{J}(u)$  is the total current operator at the time  $u$  in the Heisenberg picture, i.e.,  $\hat{J}(u) = \exp(i\mathcal{H}u)\hat{J}\exp(-i\mathcal{H}u)$ . The total current operator  $\hat{J}$  is calculated by the continuity equation of energy as  $\hat{J} = -i \sum_{\ell} \left( [\hat{h}_{\ell+1}, \hat{h}_{\ell}] + [\hat{h}_{\ell+2}, \hat{h}_{\ell}] \right)$ , using  $\hat{h}_{\ell} = J\sigma_{\ell}^z\sigma_{\ell+1}^z + D(\sigma_{\ell}^z\sigma_{\ell+1}^x - \sigma_{\ell}^x\sigma_{\ell+1}^z) + \Gamma\sigma_{\ell}^x + H\sigma_{\ell}^z$ . In order to consider the thermodynamic limit, we define  $A(t)$  and  $C(t)$  as follows,

$$A(t) = \frac{1}{2N} \langle \{ \hat{J}, \hat{J}(t) \} \rangle, \quad C(t) = \int_0^t du A(u), \quad (6)$$

where  $A(t)$  is the autocorrelation function for the total current, and  $C(t)$  is the integration of  $A(t)$ . We call  $C(t)$  the Green-Kubo integral. The numerical calculations are carried out for  $\beta = 0.3$  with the periodic boundary condition  $N_1 = N$ . In Fig. 4(a), we plotted the absolute values of the autocorrelation functions  $A(t)$  for system sizes  $N = 12, 14$  and  $16$  on the log-log scale. Up to  $N = 14$ , we used the numerical diagonalization for the Hamiltonian, and for  $N = 16$  we calculated the time evolution of wave function for the randomly chosen 1024 initial states [9]. The figure indicates the power law decay  $\sim t^{-1.5}$  of  $A(t)$ . In the inset, the raw data of  $A(t)$  for various system sizes ( $N = 8, 10, 12, 14$ , and  $16$ ) are plotted on the normal scale. All data are saturated to some finite values with fluctuations. This constant is partially caused by the energy degeneracies due to translational symmetry of periodic condition. Thus the behavior of  $A(t)$  is roughly represented as follows,

$$A(t) \sim a(N, t)t^{-1.5} + b(N, t) + B(N), \quad (7)$$

where  $a(N, t)$  and  $b(N, t)$  are some fluctuating functions with a vanishing mean value and  $B(N)$  denotes the saturated average value for  $N$ .  $B(N)$  can be exactly calculated by a numerical diagonalization up to  $N = 14$ . For  $N = 16$ , it is calculated by directly averaging the numerical data of  $A(t)$ . We find that  $B(N)$  vanishes with the increase of  $N$  following or faster than the exponential function  $0.1 \times \exp(-0.5N)$ , as shown in Fig. 4(b). There we plotted the data from  $N = 6$  to  $N = 16$ . Thus the integral  $C(t)$  is expected to converge showing roughly the

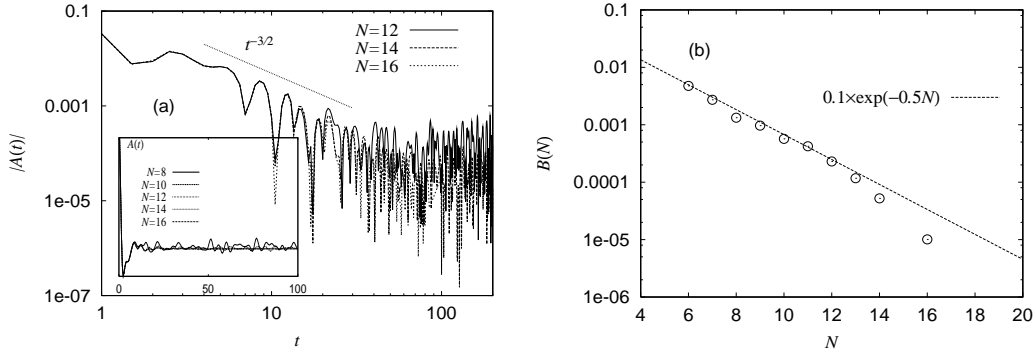


Fig. 4 – (a): The absolute values of autocorrelation function as function of time for  $N = 12, 14,$  and  $16$ . In the inset, the raw data are shown for  $N = 8, 10, 12, 14,$  and  $16$ . (b): The average constant  $B(N)$  as a function of  $N$ . The dashed line is the exponential function  $0.1 \times \exp(-0.5 \times N)$ .

following behavior in the thermodynamic limit  $N \rightarrow \infty$ ,

$$C(t) \sim \int^t a(N, u) u^{-1.5} du + B(N)t \rightarrow \int^t a(\infty, u) u^{-1.5} du < C_0 + t^{-0.5}. \quad (8)$$

In Fig.5, we present the numerically calculated  $C(t)$  for various  $N$ . The behavior of  $C(t)$  strongly supports the convergence of the Green-Kubo integral in the thermodynamic limit. The behavior of  $C(t)$  reminds us the order of limit, i.e., taking the limit  $N$  to infinity first and then  $t$  to infinity. From the convergence of  $C(t)$ , we conclude that the present one-dimensional spin system without trivial symmetries shows the finite thermal conductivity which is independent of the system size as far as  $N$  is very large.

In conclusion, we find the strong evidence of normal thermal conduction in the present system by microscopic investigation. The autocorrelation function in the Green-Kubo formula shows power law decay  $\sim t^{-1.5}$ , which may be the characteristics in the high temperature region, i.e. semiclassical region [17]. It is also interesting to study the behavior at very low temperatures. The Fig.3 indicates that this system can be the candidate which satisfies the local equilibrium. We should carefully and systematically investigate how the exponential form in the local energy distribution are realized.

In the recent experiments showing a ballistic heat transport in of  $\text{Sr}_2\text{CuO}_3$  [7] and  $\text{CuGeO}_3$  [8], the energy is transmitted by spin excitations (magnon), and the coherent length is very long (about 100 times lattice constant in  $\text{CuGeO}_3$  above the spin-Peierls temperature). Theoretical studies for temperature dependence of thermal conductivity are actively done [18,19]. It is also interesting to investigate theoretically and experimentally how the coherent length changes when the symmetries disappears in these realistic systems.

\*\*\*

The author would like to thank S. Takesue and T. Shimada for valuable discussion. He also would like to thank the valuable comments of the referees. The computer calculation was partially carried out at the computer center of the ISSP, which is gratefully acknowledged. The present work is supported by Grand-in-Aid for Scientific Research from Ministry of Education, Culture, Sports, Science, and Technology of Japan.

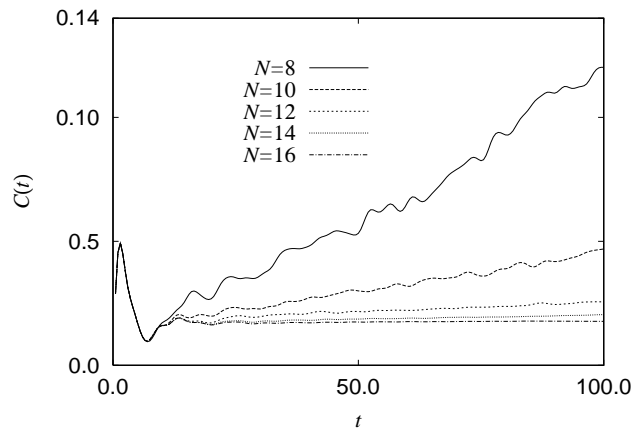


Fig. 5 – The Green-Kubo integral  $C(t)$  as a function of time for  $N = 8, 10, 12, 14$ , and  $16$ .

## REFERENCES

- [1] Z. Rieder, J. L. Lebowitz, and E. Lieb, *J. Math. Phys.* **8**, 1073 (1967), U. Zürcher and P. Talkner, *Phys. Rev. A* **42**, 3278 (1990).
- [2] S. Lepri, R. Livi, and A. Politi, *Phys. Rev. Lett.* **78**, 1896 (1997), *Europhys. Lett.* **43**, 271 (1998).
- [3] K. Saito, S. Takesue, and S. Miyashita, *Phys. Rev. E* **54**, 2404 (1996).
- [4] K. Saito, S. Takesue, and S. Miyashita, *Phys. Rev. E* **61**, 2397 (2000).
- [5] A. Lippi, R. Livi, *J. Stat. Phys.* **100** 1147 (2000), T. Shimada, T. Murakami, S. Yukawa, K. Saito, and N. Ito, *J. Phys. Soc. Jpn* **69** 3150 (2000).
- [6] P. Mazur, *Physica* **43** 533 (1969), X. Zotos, F. Naef and P. Prelovsek, *Phys. Rev. B* **55**, 11029 (1997).
- [7] A.V.Sologubenko, K. Gioannó, H. R. Ott, A. Vietkine, and A. Revcolevschi, *Phys. Rev. B* **62** R6108 (2000), *Phys. Rev. B* **64** (2001) 054412-1.
- [8] Y. Ando, J. Takeya, D. L. Sisson, S. G. Doettinger, I. Tanaka, R. S. Feigelson, and A. Kapitulnik, *Phys. Rev. B* **58** R2913 (1998).
- [9] T. Prosen, *Phys. Rev. Lett.* **80** 1808 (1998), *Phys. Rev. E* **60** 3949 (1999).
- [10] G. Jona-Lasinio and C. Presilla, *Phys. Rev. Lett.* **77** 4322 (1996).
- [11] S. Katsura, *Phys. Rev.* **127** 1508 (1962).
- [12] For example, in the free fermion case of  $D = H = 0$ , the fermion can run through without scatterings, which causes the ballistic transport. In that case, the temperature profile becomes flat [3].
- [13] O. Bohigas, M.-J. Giannoni, and C. Schmit, *Phys. Rev. Lett.* **52**, 1 (1984), M. V. Berry and M. Tabor: *J. Phys. A* **10** (1977) 371.
- [14] We regard the system (1) as a dynamical model which shows a variety of complex dynamics. We take this simple set of parameters although the DM interaction is relatively large.
- [15] K. Saito, S. Takesue, and S. Miyashita, *Phys. Rev. E* **59** 2783 (1999).
- [16] A. Dhar, *Phys. Rev. Lett.* **86** 3554 (2001).
- [17] T. Prosen, *Progr. Theor. Phys. Suppl.* **139** 191 (2000).
- [18] A. Klümper and K. Sakai, *J. Phys. A* **35** (2002) 2173.
- [19] K. Saito, and S. Miyashita, *J. Phys. Soc. Jpn* **71** (2002) 2485.